Article

Understanding the Transient Microwave Drying Performances of Industrial Sewage Sludge Towards Green Fuel and Energy

Kaihan Xie [1], Zhihong Liu [1], Man Zhang [2,*], Wenke Zhao [1] and Yaning Zhang [1,*]

[1] School of Energy Science and Engineering, Harbin Institute of Technology, Harbin 150001, China
[2] Key Laboratory for Thermal Science and Power Engineering of Ministry of Education, Department of Energy and Power Engineering, Tsinghua University, Beijing 100084, China
* Correspondence: zhangman@mail.tsinghua.edu.cn (M.Z.); ynzhang@hit.edu.cn (Y.Z.)
Received: 3 May 2025; Revised: 28 June 2025; Accepted: 2 July 2025; Published: 8 July 2025

Abstract: Drying treatment, as a critical initial processing step, enables the transformation of industrial sewage sludge into green fuels, addressing dual environmental and energy challenges. A designed microwave drying thermogravimetric experimental system was developed to investigate the effects of sludge weight (20, 25, 30, 35, and 40 g) and microwave power (400, 450, 500, 550, and 600 W) on the drying performances through analysis of transient temperature and weight. Results identified three distinct drying stages: (I) rapid preheating dominated by sensible heat absorption of free water; (II) constant-temperature stage where microwave energy primarily converted to latent heat for free water removal; (III) slower bound-water removal stage. Crucially, drying performance peaked at 30 g sludge weight. Increasing microwave power significantly enhanced efficiency, reducing total drying time by 37.4% when power rose from 400 W to 600 W. Maximum drying efficiency (81.9 wt.% moisture removal) occurred at 500 W, demonstrating a non-linear power-efficiency relationship. These findings provide essential mechanistic insights and operational parameters to optimize industrial sludge to energy processes.

Keywords: microwave drying; industrial sewage sludge; transient thermogravimetry; weight; temperature

1. Introduction

The continuous progress of industrialization and urbanization has led to a substantial annual increase in global industrial sewage sludge (ISS) generation [1]. Current worldwide production of dry ISS reaches approximately 1.6 million tons per year [2], presenting a significant environmental challenge.

Figure 1 shows the main components and utilization methods of ISS. There are substantial organic constituents in the ISS, demonstrating significant potential as a renewable source for green fuels and energy production [3,4]. ISS can be converted into green fuels and energy through various methods, including anaerobic digestion [5], pyrolysis [6], gasification [7], combustion [8], and composting [9]. Notably, ISS biochar shows potential applications in soil remediation [10] and water treatment [11]. These approaches enable simultaneous waste management and green energy generation while addressing environmental concerns associated with ISS disposal.

However, due to the characteristic of ISS having an ultra-high moisture content [12], it is necessary to perform drying treatment to effectively reduce the costs of transportation and storage [13], as well as the energy consumption of subsequent processing [14]. For instance, Zhang et al. [15] investigated a 400 t/d sludge thermal drying-combustion pilot plant. Their research revealed that the energy required for the drying process significantly decreased as the sludge moisture content was reduced. When the sludge moisture content decreased from 80% to 50%, the recoverable energy from the combustion process increased from 3213.49 to 8047.5 kW.

The widely adopted ISS drying methods include pressure filtration drying [16], hot air heating drying [17], solar drying [18] and microwave drying [19]. Pressure filtration drying utilizes a filter press to mechanically dewater ISS. While this method requires no thermal energy input, its dehydration capability is limited to reducing moisture content to 80% of the initial value [20]. Hot air drying achieves sludge dewatering by utilizing heated air streams. Currently, hot air is typically sourced from direct electric heating or biomass combustion [21,22]. Despite advantages in operational simplicity and technological maturity, its fundamental dependence on external-to-internal thermal conduction in samples inevitably leads to limitations: high energy consumption from low thermal

penetration efficiency [23], material surface scorching caused by localized heating, and unsatisfactory drying rates [24]. Solar drying utilizes thermal energy derived from solar radiation to dewater ISS, representing a cost-effective and environmentally benign dewater method. Currently, solar drying systems can be classified into two principal categories: direct solar drying [25] and concentrated solar drying [26,27]. Under conditions of insufficient solar irradiance, concentrated solar drying systems demonstrate enhanced efficacy in improving drying efficiency.

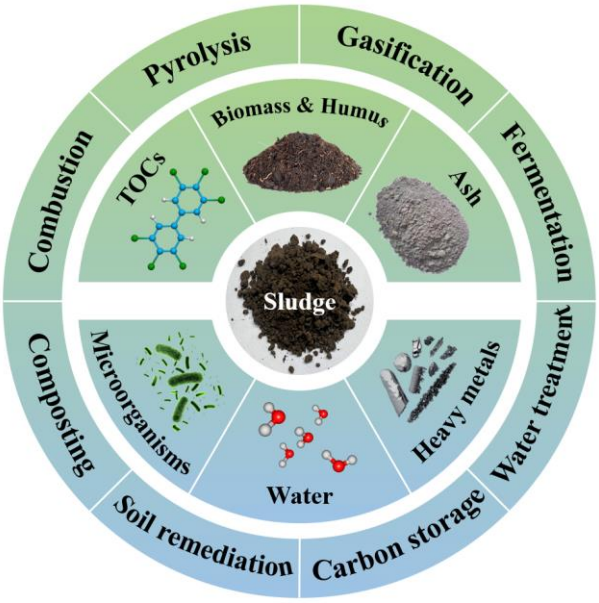

Figure 1. Main components and utilization methods of ISS.

Microwave drying involves the conversion of electrical energy into microwave radiation, which is subsequently utilized to heat the ISS. Microwave, defined as non-ionizing electromagnetic radiation with a frequency range from 300 MHz to 300 GHz and a wavelength between 1 mm and 1 m, possesses the ability to penetrate materials with ease [28]. The primary heating mechanisms of microwave are dipole rotation and ionic polarization [29]. As microwave radiation interacts with the dipoles within a material, it induces high-speed rotation. This rapid rotation, coupled with the resulting collisions between dipoles and surrounding molecules, amplifies molecular vibrations, generating frictional heat that raises the temperature of the substance [30]. Consequently, due to the superior uniformity and energy efficiency of microwave radiation, microwave drying outperforms alternative dehydration methods in achieving rapid and uniform drying of ISS [31].

Microwave drying offers a more efficient and uniform drying method. In recent years, the advantages of microwave drying have been increasingly recognized, leading to a growing body of research on this technique. Ozdemir et al. [32] investigated the effects of microwave drying on propolis extract, demonstrating that increasing the microwave power from 180 to 900 W reduced the drying time by 67%. Furthermore, at 900 W, the propolis extract exhibited the highest effective moisture diffusivity, with its phenolic and flavonoid contents being comparable to those of fresh propolis extract, indicating the most effective drying conditions. Carvalho et al. [33] compared the differences between electric heating drying and microwave drying for barley malt. The results revealed that traditional electric heating drying required 540–840 min, while microwave drying reduced the time by 95%. Meanwhile, microwave drying technology has also been applied to sludge drying. Wang et al. [34] studied the drying characteristics of chromium-rich electroplating sludge, showing that the sludge exhibited excellent microwave absorption. Compared to conventional drying at 105 °C, microwave drying at 600 W reduced the drying time by 98.5%. Slezak et al. [35] investigated the effects of microwave power and drying time on the drying performance using fine dust sludge with a moisture content of 26–60%. The experimental results demonstrated that microwave drying at 300 W for 6 min represented the optimal condition. However, the application of excessively high microwave power was observed to induce vigorous boiling of the material during the drying process, which, under extreme circumstances, could result in the explosive disintegration of the sample. Wulyapash et al. [36] conducted a comparative analysis between hot air drying and microwave drying, revealing that microwave drying could reduce the drying time by 37.5%. The total calorific value of sludge dried by microwave ranged from 20.8 to 21.4 MJ/kg, while that of sludge dried by hot air ranged from 19.4 to 21.8 MJ/kg, indicating that microwave drying does not adversely affect the calorific value of the sludge.

However, current research predominantly focuses on analyzing drying results [37–39], but lacks investigation into transient temperature and weight loss. This gap makes it difficult to gain deeper insights into the transient drying performances of sludge and conduct kinetic and thermodynamic analysis. Therefore, this study developed a microwave drying thermogravimetric experimental system to investigate the effects of ISS weight and microwave power on the drying performance by analyzing the transient variations in ISS temperature and weight during the drying process.

2. Materials and Methods

2.1. Materials

The ISS sample utilized in this study was sourced from Qingdao Tundao Sewage Treatment Plant (Qingdao, Shandong, China). Before the drying experiment, all ISS samples were crushed into particles less than 3 mm. The photographs of ISS sample and ISS particles after sieving were shown in Figure 2.

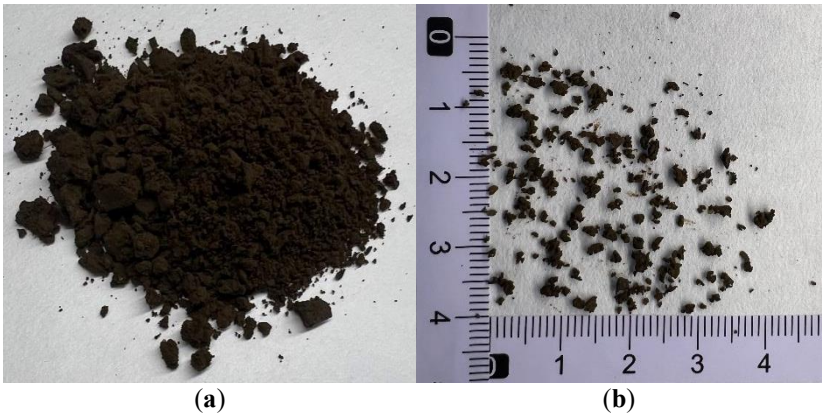

Figure 2. Photographs of (**a**). ISS sample and (**b**) ISS particles after sieving.

2.2. Experimental Setup

Figure 3 illustrates the experimental setup used to explore the drying effect of ISS. Figure 4 displays a photograph of the microwave drying experimental system. The experimental setup comprised a microwave oven, an iron support, a tension sensor, two data acquisition instruments, a thermocouple, a heating band, a fan and a reactor.

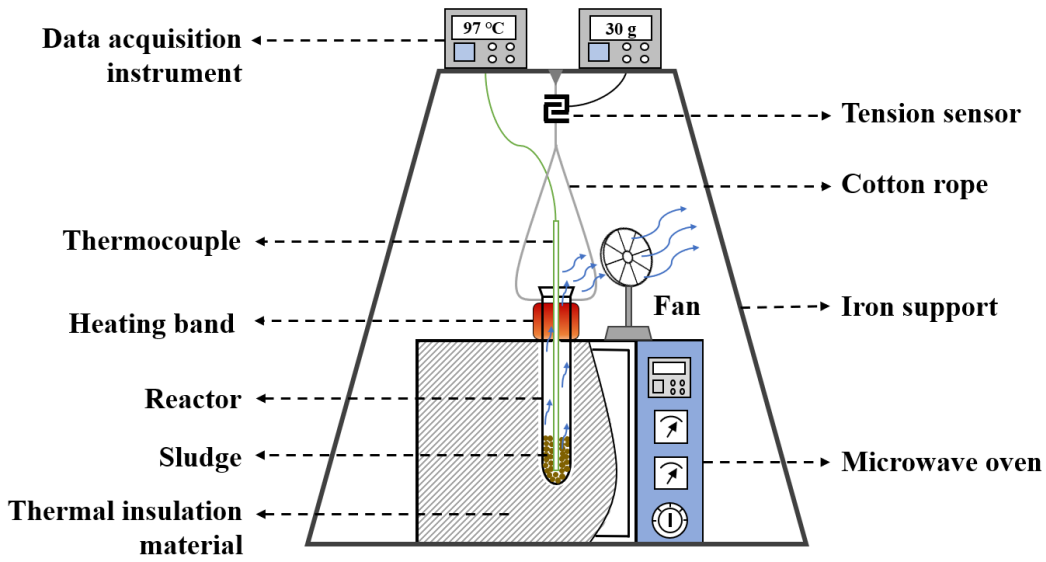

Figure 3. Schematic diagram of the microwave drying experimental system.

The laboratory-scale microwave oven procured from Shanghai Longyu Microwave Equipment Company (Shanghai, China) delivers a fixed 2.45 GHz output frequency with power adjustable via rotary knob (300–1000 W), while real-time monitoring ensured operational consistency between actual and preset power values. The microwave chamber was constructed from stainless steel. After closing the chamber door, aluminum foil tape was applied to seal

the door gaps, effectively preventing any microwave leakage. The reactor was a quartz tube with an outer diameter of 26 mm, a wall thickness of 2 mm, and a length of 300 mm. The thermal insulating material was aluminosilicate ceramic fiber, which did not absorb microwaves. The microwave chamber was fully filled with the insulating material, but the material did not come into contact with the reactor to avoid affecting the experimental results.

Sample weight was measured using a tension sensor procured from Bengbu Sensor Systems Engineering Co., Ltd. (Anhui, China), featuring a 0–500 g measurement range with measurement error not exceeding ±0.25 g. Temperature was monitored via a PT100 thermocouple procured from Sanping Hardware Equipment Co., Ltd. (Shanghai, China), with a measurement range of 0–600 °C and an accuracy specification of ±0.1 °C. The temperature and weight of ISS were recorded separately by two data acquisition instruments every 1 s. The iron support was heavy enough to effectively prevent errors caused by vibration. The heating band was set to 90 °C, which ensured no vapor would liquefy at the top of the reactor. The fan was used to change the direction of vapor and prevent it from interfering with the tension sensor.

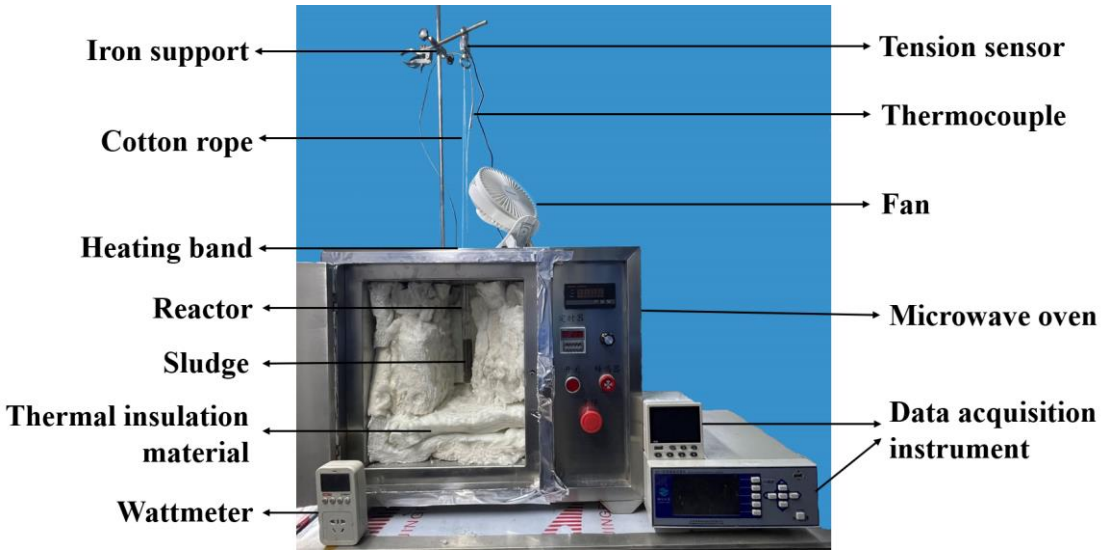

Figure 4. Photograph of the microwave drying experimental system.

2.3. Experimental Procedures

The detailed experimental procedures are as follows:

(1) The ISS blocks were crushed using a mortar and sieved to obtain particles with a diameter less than 3 mm.
(2) A measured quantity of ISS was introduced into the reactor. Void spaces between particles were minimized by gentle tapping of the vessel walls. A thermocouple was inserted and positioned 10–15 mm above the reactor base.
(3) The reactor was coupled to a tension sensor via a cotton rope linkage, and the assembly height was adjusted. Residual volume within the microwave chamber was occupied with thermal insulation material. The seams of microwave oven were sealed using aluminum foil tape to mitigate microwave leakage.
(4) Electrical heating band was activated and regulated to a setpoint temperature of 90 °C. The fan and data acquisition instruments were turn on. Temperature and mass data were sampled at one second intervals by the data acquisition instruments. Once the system stabilized, the microwave oven was initiated to begin the experiment.
(5) As temperature increased, upon reaching 110 °C, microwave power was modulated to maintain this temperature for a duration of 6 min.
(6) Subsequent to the isothermal period, heating was continued. Microwave irradiation was discontinued upon the sample temperature attaining 150 °C.

2.4. Data Analysis

The weight loss rate and average heating rate were calculated to analysis drying effect. The detailed equations were:

$$R_W = \frac{m_1 - m_2}{m_0} \times 100\% \quad (1)$$

$$R_H = \frac{T_2 - T_1}{t_2 - t_1} \times 100\% \quad (2)$$

where:

R_W, is weight loss rate, wt.%.
m_0, is the initial weight of the sample, g.
m_1, is the weight of the sample at point 1, g.
m_2, is the weight of the sample at point 2, g.
R_H, is the average heating rate, °C/min.
T_1, is the temperature of the sample at point 1, °C.
T_2, is the temperature of the sample at point 2, °C.
t_1, is the time of the sample at point 1, min.
t_2, is the time of the sample at point 2, min.

3. Results and Discussion

3.1. Effect of ISS Weight

This section focused on studying the effect of ISS weight (20, 25, 30, 35, and 40 g) on the drying efficiency. A microwave power of 500 W was used. When the drying temperature reached 110 °C, the process was halted after 6 min to enhance the drying effect.

3.1.1. Transient Temperature

Figure 5 illustrates the transient temperature variations of ISS with different weights. The drying process commenced at an initial temperature of 15 °C and concluded at 150 °C. The figure reveals three distinct drying stages: (I) preheating stage, (II) constant-temperature drying stage, and (III) falling-rate drying stage.

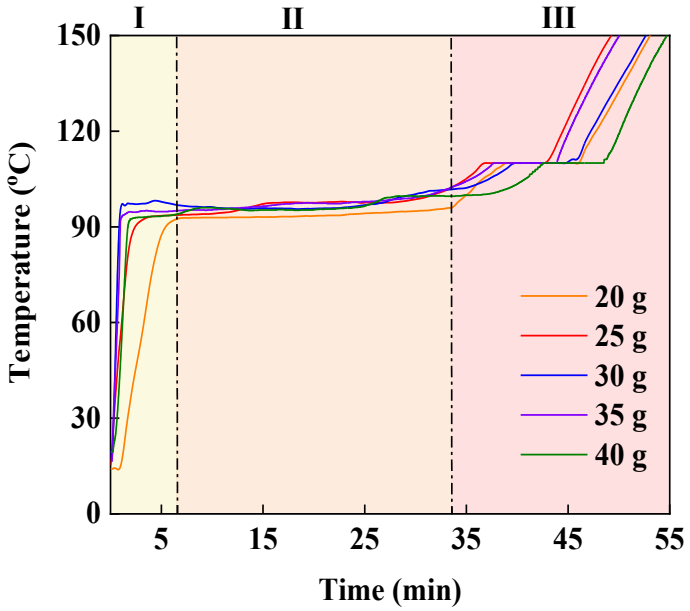

Figure 5. Curve of transient temperature variations with different weights at 500 W.

Table 1 summarizes the average heating rates of ISS samples with different weights during each stage. It is evident that all five ISS samples exhibited significantly higher average heating rates during stage (I). The average heating rate initially increased with sample weight, and subsequently decreased. Specifically, the 20 g sample demonstrated the lowest average heating rate of 19.33 °C/min, whereas the 30 g sample achieved the highest rate of 120.02 °C/min. A progressive enhancement in microwave absorption was observed as sample weight increased from 20 to 30 g. This elevation corresponded directly to increased thermal energy acquisition per unit time, resulting in accelerated average heating rates. Beyond the 30 g, samples approached near-total microwave absorption, leading to no further increase in heat acquisition per unit time. The substantial water content in samples combined with water's high specific heat capacity caused the average heating rate to decrease with continued weight increase. During this stage, the microwave energy absorbed by the samples was predominantly converted

into sensible heat of the water within the ISS [34]. Concurrently, the vapor pressure of the water in the ISS increased progressively with rising temperature [40].

When the sample temperature reached 90–100 °C, and the vapor pressure of the water equaled the ambient pressure, the drying process transitioned into stage (II) [39]. During this stage, the temperature of all samples remained below 100 °C, as the absorbed microwave energy was not only utilized for the latent heat of stage change of the liquid water in the ISS but was also partially dissipated into the surrounding environment. The limited microwave energy was insufficient to sustain the ISS temperature at 100 °C [41]. The heating rates of all samples were relatively low, ranging from 0.20 to 0.30 °C/min, except for the 20 g ISS sample, which exhibited a heating rate of only 0.11 °C/min. The slowed heating rate resulted from impaired microwave energy coupling efficiency. This impairment occurred because at 20 g ISS sample weight, the low filling ratio in the reactor yields a reduced projected area, consequently causing inadequate absorption of microwave irradiation [42,43].

Upon the removal of the majority of free water from the samples, the temperature began to rise, marking the onset of stage (III). Following the constant-temperature stage, the heating curves of all samples tended to become parallel, with the average heating rates of the five sample groups reaching 5.61, 6.14, 6.16, 6.13, and 6.23 °C /min respectively.

Table 1. Average heating rates of ISS with different weights (°C/min).

Weight	Stage I	Stage II	Stage III
20 g	19.33	0.11	5.61
25 g	41.74	0.26	6.14
30 g	120.02	0.20	6.16
35 g	75.51	0.22	6.13
40 g	36.13	0.21	6.23

3.1.2. Transient Weight

Figure 6 demonstrates the transient weight variations of ISS samples with different weights. As shown in the figure, the weight loss process can also be divided into three distinct stages, corresponding to the temperature variation stages. During stage (I), except for the 20 g ISS group, the drying rates of the remaining four groups exhibited the highest values among all three stages. This phenomenon can be attributed to two factors. (1) In the initial drying stage, the ISS contains a substantial amount of free water [44], whose molecules readily rotate under the oscillating magnetic field generated by microwave radiation, generating heat through molecular friction [45]. (2) During the early heating stage, the moisture on the ISS surface is directly exposed to the ambient air, resulting in minimal evaporation resistance. Additionally, microwave heating induces rapid internal temperature elevation, increasing the water vapor pressure and creating a significant pressure gradient between the ISS interior and the external environment, thereby accelerating moisture removal [46]. In contrast, the 20 g ISS group demonstrated limited weight loss in stage (I) due to incomplete microwave absorption and slower heating rates.

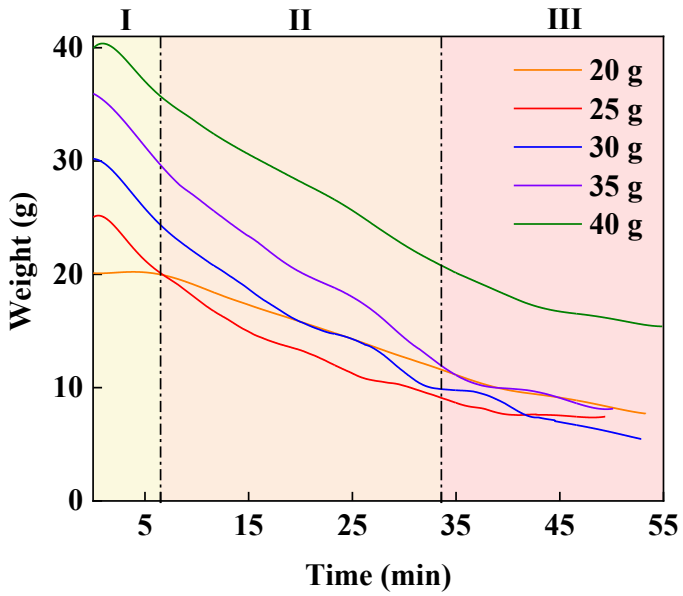

Figure 6. Curve of transient weight variations with different weights at 500 W.

In stage (II), all groups exhibited significant weight loss, corresponding to the primary evaporation stage of free water. The cumulative weight losses of the five groups reached 8.4, 11.0, 14.5, 17.7, and 18.05 g, accounting for 42.0 wt.%, 44.0 wt.%, 48.3 wt.%, 50.6 wt.%, and 45.1 wt.%, respectively. Notably, the 40 g ISS group required an extended stage (II) duration of 43 min to complete free water removal due to its higher initial weight.

As the drying process proceeded, the moisture content of the ISS further decreased, leading to a decline in drying rate and the transition to stage (III). During this stage, the five sample groups achieved weight reductions of 19.4 wt.%, 7.16 wt.%, 14.7 wt.%, 11.0 wt.%, and 13.6 wt.%, respectively. The weight loss was primarily governed by the evaporation of bound water, with moisture migration dominated by internal diffusion mechanisms [47]. Concurrently, progressive surface hardening and partial pore clogging in the ISS increased weight transfer resistance [48].

3.1.3. Thermogravimetric Analysis

Figure 7 shows the thermogravimetric curves of five ISS samples. It is evident from the figure that below 90 °C, the sample mass remained almost unchanged with increasing temperature. This indicated that during this stage, the microwave radiation energy was converted into the internal energy of the samples, with almost no moisture removal occurring. However, a significant weight loss was observed in the temperature range of 90–100 °C. This finding corresponds exactly to stage (II) of the microwave drying process shown in Figures 5 and 6, where slow temperature increases and substantial mass reduction occurred simultaneously. This further verified that during stage (II), the absorbed microwave radiation energy was converted into the latent heat of water and the energy required for moisture transport. At 100 °C, the cumulative weight losses of the five groups reached 44.4 wt.%, 61.3 wt.%, 61.5 wt.%, 62.5 wt.%, and 51.1 wt.%, respectively. Beyond 100 °C, the weight loss rate per unit temperature gradually decreased. A sharp decline in sample weight was observed at 110 °C, resulting from the 6-min isothermal holding at this temperature. Following the isothermal stage, minimal weight variations were detected in the four groups with ISS weights above 20 g as temperature increased, indicating that the majority of bound water had been removed. Upon reaching 150 °C, the total weight losses of the five groups were 61.4 wt.%, 70.2 wt.%, 81.9 wt.%, 76.7 wt.%, and 61.5 wt.%, respectively. These results indicate that the effectiveness of microwave drying initially increased and subsequently decreased with increasing ISS weight, achieving optimal performance at 30 g.

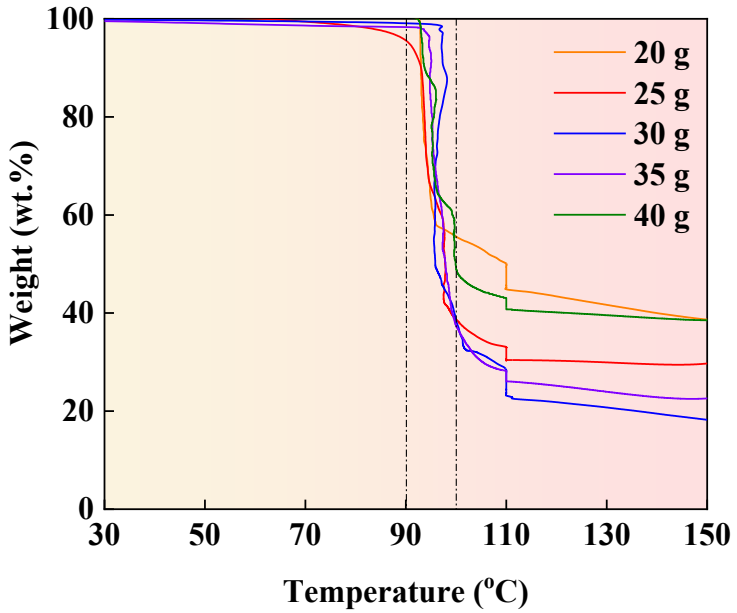

Figure 7. Thermogravimetric curve of ISS with different weights at 500 W.

3.2. Effect of Microwave Power

In Section 3.1, a raw material weight of 30 g resulted in the highest weight loss for the ISS samples. Therefore, this section is dedicated to examining the influence of microwave power (400, 450, 500, 550, and 600 W) on drying performance. The raw material weight was fixed at 30 g, and an isothermal holding period of 6 min at 110 °C was maintained to optimize drying efficiency.

3.2.1. Transient Temperature

Figure 8 presents the variation in the transient temperature of the ISS samples under different microwave powers. As depicted in the figure, following the initiation of heating, the temperature of the samples exhibited a rapid increase from ambient temperature to 90–100 °C, after which it stabilized for a brief period before continuing to rise. The overall process can be categorized into three distinct stages. Notably, when the microwave power was set to 400 W, the drying time was markedly longer compared to the other four power settings. Upon increasing the microwave power from 400 W to 600 W, the time required for the sample to reach 150 °C decreased from 67.9 to 42.5 min, resulting in a reduction of 25.4 min. This reduction is attributed to the intensified vibration of polar molecules within the ISS, which, as the microwave power increased, led to a higher generation of heat.

In stage (I), the increase in microwave power had a negligible effect on the heating rate, as all five sample groups reached 90–100 °C within a very short period. In stage (II), the temperature of the samples in all groups remained largely below 100 °C. During this stage, the energy input from the microwave radiation was primarily converted into the latent heat of stage transition of the free water within the ISS. Among these, the sample exposed to 550 W of microwave power exhibited a superheating phenomenon, where the temperature first increased and then decreased, with a maximum temperature reaching 106.7 °C. This phenomenon is due to the generation of excessive water vapor under high microwave power, which could not be expelled quickly enough. As a result, the pressure difference between the surface and internal steam increased, causing superheating [39].

As the drying process progressed into stage (III), the temperature of the samples rose again. At this point, most of the free water had been removed, leaving behind primarily bound water and solid ISS. The average heating rates of the samples during this stage were significantly influenced by the microwave power. The average heating rates from 110 to 150 °C for the five groups of samples were 4.22, 3.91, 5.59, 5.66, and 12.08 °C/min, respectively. This variation can be attributed to that part of the absorbed microwave energy was used as latent heat to evaporate the bound water, while the remaining energy served as sensible heat to raise the temperature of the ISS solids.

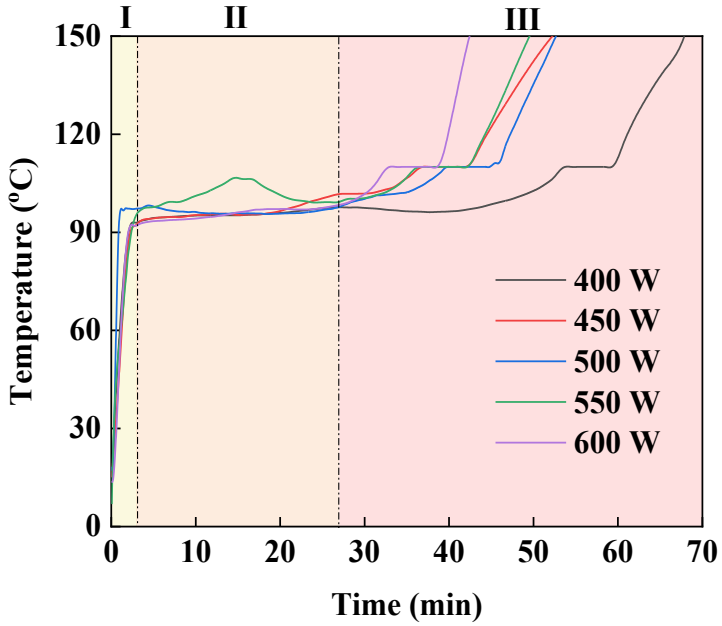

Figure 8. Curve of transient temperature with different microwave power at 30 g ISS.

3.2.2. Transient Weight

Figure 9 presents the variation in the transient weight of the ISS samples under different microwave powers. As shown in the figure, the weight change can also be divided into three stages, corresponding to the stages of temperature change. Due to the rapid heating rates in all five sample groups, the weight change was minimal in stage (I). Stage (II) represented the primary stage of weight loss. During this stage, the average weight loss rate of the five sample groups increased with the rise in microwave power. The highest average weight loss rate was observed when the microwave power was 600 W. Additionally, for the sample exposed to 550 W microwave power, a notable change in the weight loss rate was observed at 18.9 min. This coincided with the time at which the sample in Figure 7 reached its maximum superheating temperature of 106.7 °C, indicating that the superheating phenomenon in the early drying stage may facilitate the removal of free water. Once the drying process entered stage (III), the rate of weight loss decreased, and the removal of bound water became the dominant process.

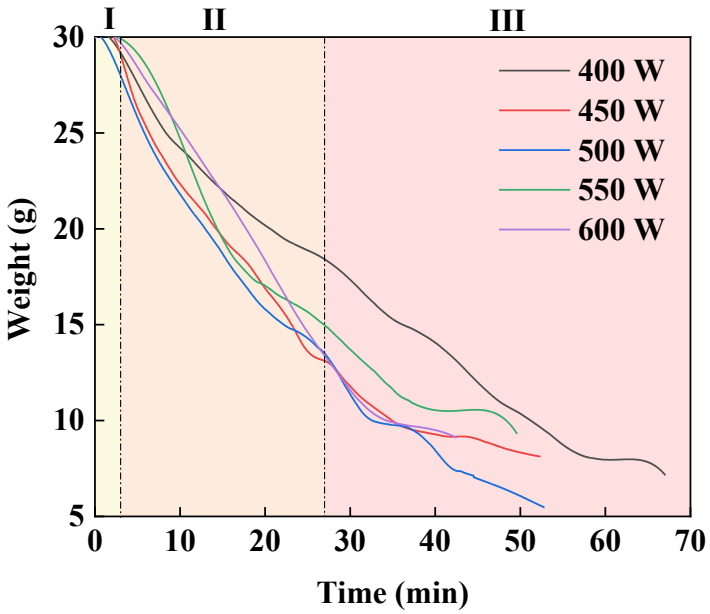

Figure 9. Curve of transient weight with different microwave power at 30 g ISS.

3.2.3. Thermogravimetric Analysis

Figure 10 shows the thermogravimetric curve of the five ISS samples with respect to microwave power. As can be clearly seen from the figure, all five sample groups exhibited the highest weight loss rates during the temperature rise from 90 to 100 °C. At 100 °C, the cumulative weight loss for the five groups were 63.3 wt.%, 53.6 wt.%, 61.5 wt.%, 51.3 wt.%, and 59.0 wt.%, respectively. After the temperature exceeded 100 °C, the weight loss rate per unit temperature gradually decreased. Following the constant temperature stage, all five sample groups showed minimal changes in weight with increasing temperature, indicating the substantial removal of bound water from these samples. This conclusion is supported by data presented in Figures 8 and 9. Specifically, Figure 8 demonstrates that once sample temperatures exceeded 110 °C, the average heating rates became comparable across all groups and increased significantly relative to pre-constant temperature stage values, reflecting consistently low residual bound water content. Figure 9 shows negligible weight variations over time after the constant temperature stage concluded, further corroborating that minimal bound water remained. When the temperature reached 150 °C, the cumulative weight losses of the five groups were 76.7 wt.%, 72.9 wt.%, 81.9 wt.%, 68.5 wt.%, and 69.67 wt.%, respectively. This indicated that the effect of microwave drying on the ISS initially increased with microwave power and then decreased, reaching its optimum at 500 W.

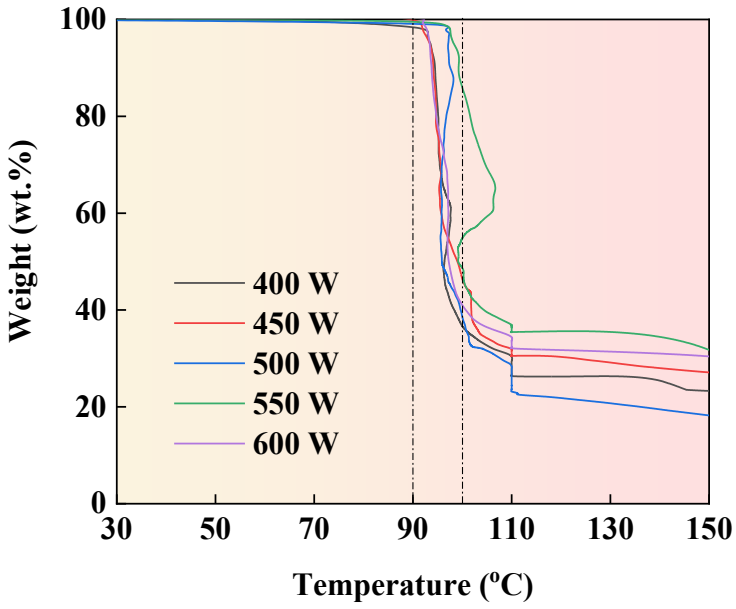

Figure 10. Thermogravimetric curve with different microwave power at 30 g ISS.

3.3. Mechanism of Microwave Drying

Microwave drying utilizes the ability of microwaves to induce rapid rotation of polar molecules within a material. This intensifies molecular collisions and friction, causing the temperature of the substance to rise continuously. Figure 11 illustrates the mechanism of microwave drying. The diagram shows that when the ISS material is placed in a microwave environment, the continuous heating by the microwaves causes the water in the ISS to convert into vapor. This vapor then escapes from the ISS, achieving the drying effect.

The process occurs as follows. When microwave radiation penetrates ISS, polar water molecules (including free and bound water) undergo rapid rotation, leading to rapid heat accumulation. As depicted in stage I of Figures 5 and 8, temperature of ISS increases sharply during the initial heating phase.

As the temperature of the ISS increases, the kinetic energy of the water molecules gradually rises. Free water is primarily influenced by hydrogen bonds and van der Waals forces. These forces result in relatively weak intermolecular interactions, and the water molecules are not strongly adsorbed by the solid particles in the ISS. As the temperature approaches water's boiling point, free water molecules acquire sufficient kinetic energy to overcome intermolecular forces and undergo rapid evaporation. This is evidenced in stage II of Figures 5 and 8, where the ISS temperature plateau occurs at 90–100 °C with minimal temperature increase. Concurrently, distinct mass loss is observed in stage II of Figures 6 and 9. These phenomena confirm that microwave energy is primarily consumed by free water evaporation at this stage, rather than sensible heating.

Bound water is influenced not only by hydrogen bonds and van der Waals forces but also by electrostatic forces, capillary forces, and other interactions. As a result, bound water does not evaporate as quickly as free water during microwave heating. Only as the temperature increases further, and the bound water molecules acquire greater kinetic energy, can they overcome the adsorption forces or chemical bonds with the solid particles in the ISS. This results in the eventual release of bound water. As evidenced in stage III of Figures 6 and 9, when ISS temperature exceeds 100 °C, persistent mass loss continues despite minimal temperature elevation, indicating thermal decomposition of sludge constituents.

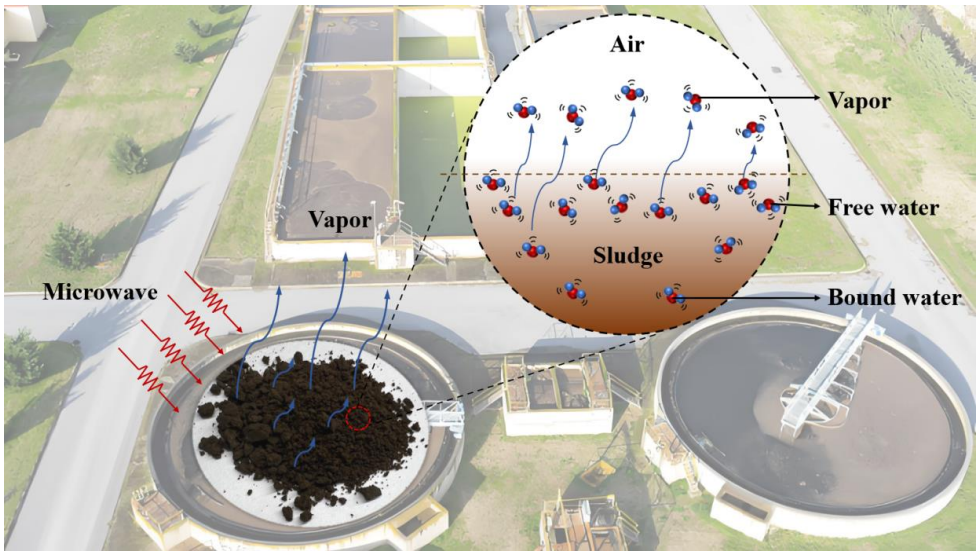

Figure 11. Mechanism diagram of microwave drying.

4. Conclusions

The transient microwave drying performances of ISS at different ISS weights (20, 25, 30, 35, and 40 g) and microwave powers (400, 450, 500, 550, and 600 W) studied and presented. Some conclusions were obtained.

The ISS drying process can be divided into three stages: (I) preheating stage, (II) constant-temperature drying stage, and (III) falling-rate drying stage. In stage (I), the microwave energy absorbed by the sample was mainly converted into sensible heat to raise the temperature of the free water in the sample, which was reflected in the rapid temperature rise and minimal weight loss. In stage (II), microwave energy was primarily converted into latent heat of stage transition of the free water in the sample, leading to the temperature remaining between 90 and 100 °C while the weight of the sample decreased significantly. In stage (III), the free water in the sample was almost completely removed, and microwave energy was converted into the latent heat of stage transition of the bound water and the sensible heat of the ISS particles, characterized by a slow rise in temperature and gradual weight loss.

The drying performance of ISS increased with the ISS weight up to a peak at 30 g, after which it decreased. At the end of the drying process, the cumulative weight losses for the five ISS weights were 61.4 wt.%, 70.2 wt.%, 81.9 wt.%, 76.7 wt.%, and 61.5 wt.%, respectively. When the microwave power increased from 400 W to 600 W, the total drying time was reduced by 37.4%. At the end of the drying process, the cumulative weight losses for the five microwave powers were 76.7 wt.%, 72.9 wt.%, 81.9 wt.%, 68.5 wt.%, and 69.67 wt.%, respectively. The optimal microwave drying performance was at 30 g ISS weight and 500 W microwave power.

Author Contributions: K. X.: writing—original draft preparation; Z. L.: data curation; M. Z.: supervision; W. Z.: software, validation; Y. Z.: supervision. All authors have read and agreed to the published version of the manuscript.

Funding: This research was funded by the National Natural Science Foundation of China (52476005, 52076049), Heilongjiang Province "Double First-class" Discipline Collaborative Innovation Achievement Project (LJGXCG2023-080), Heilongjiang Provincial Key R&D Program (2023ZX02C05), and Heilongjiang Provincial Key R&D Program "Unveiling the Leader" Project (2023ZXJ02C04).

Institutional Review Board Statement: Not applicable.

Informed Consent Statement: Not applicable.

Data Availability Statement: Data will available on request.

Conflicts of Interest: The authors declare no conflict of interest.

References

1. Guo. H.Y.; Tan, Z.W.; Li, H.Y.; et al. Dynamic characteristics analysis of metallurgical waste heat radiative drying of thin layers of sewage sludge. *Processes* **2023**, *11*, 2535.
2. Feng, J.I.; Burke, T.; Chen, X.; et al. Assessing metal contamination and speciation in sewage sludge: Implications for soil application and environmental risk. *Rev. Environ. Sci. Bio.* **2023**, *22*, 1037–1058.
3. Wang, L.P.; Chang, Y.Z.; Li, A. Hydrothermal carbonization for energy-efficient processing of sewage sludge: A review. *Renew. Sust. Energ. Rev.* **2019**, *108*, 423–440.
4. Li, Y.D.; Yang, D.; Zhou, X.H.; et al. Heavy metal migration characteristics of co-combustion between sewage sludge and high alkaline coal on circulating fluidized bed. *J. Therm. Sci.* **2022**, *31*, 2178–2188.
5. Nwankwo, N.C.; Madougou, S.; Inoussa, M.M.; et al. Review of Nigeria's renewable energy policies with focus on biogas technology penetration and adoption. *Discov. Energy* **2024**, *4*, 14.
6. Li, Q.; Zhong, Z.Q.; Du, H.R.; et al. Co-pyrolysis of municipal sludge and papermaking sludge: Pyrolysis behaviors and heavy metals immobilizations. *J. Anal. Appl. Pyrol.* **2024**, *181*, 106595.
7. Jiang, S.Y.; Du, Y.; Li, Y.J.; et al. Crystal facet effect of the support in Ni/$La_2O_2CO_3$ catalysts for toluene steam reforming. *Fuel* **2025**, *387*, 134388.
8. Ji, X.L.; Yang, Q.Y.; Huang, X.Y.; et al. Combustion characteristics and NO_x release of sludge combustion with coal in a 660 MW boiler. *Appl. Therm. Eng.* **2024**, *258C*, 124749.
9. Cheng, D.M.; Xiong, J.S.; Chen, J.Y.; et al. Effect of biochar addition on antibiotic and heavy metal resistance genes during sewage sludge composting. *J. Environ. Chem. Eng.* **2025**, *13*, 115732.
10. Jin, F.Y.; Lu, J.X.; Sun, F.; et al. Application and development of sludge-based materials for environmental pollution remediation: A bibliometric review from 2004 to 2024. *RSC Adv*. **2025**, *15*, 8072–8087.
11. Mian, M.M.; Ao, W.Y.; Deng, S.B. Sludge-based biochar adsorbent: Pore tuning mechanisms, challenges, and role in carbon sequestration. *Biochar* **2023**, *5*, 83.
12. Laghari, A.A.; Leghari, A.; Kumar, A.; et al. A parametric study of particle size influence on sewage sludge-derived hydrochar and coal char co-gasification: Reactivity and carbon conversion analysis. *Biomass Bioenergy* **2025**, *196*, 107715.
13. Quan, L.M.; Kamyab, H.; Yuzir, A.; et al. Review of the application of gasification and combustion technology and waste-to-energy technologies in sewage sludge treatment. *Fuel* **2022**, *316*, 123199.
14. Jiang, Y.F.; Gao, F.Y.; Peng, G.D.; et al. Effect of carbon to nitrogen ratios of municipal sludge on its dehydration property. *Energ. Source Part A* **2023**, *45*, 2509–2522.
15. Zhang, K.B.; Yu, A.B.; He, X.H.; et al. Process simulation and techno-economic analysis of 400 t/d pilot plant for municipal sewage sludge drying and combustion. *Process Saf. Environ.* **2025**, *196*, 106833.
16. Mariusz, K.; Tomasz, K. Increase in efficiency of separating pollution from sewage sludge through the pressure filtration process. *Desalin. Water Treat.* **2023**, *301*, 181–189.
17. Wang, G.Y.; Wu, W.F.; Qiao, F.X.; et al. Research on an electric energy-saving grain drying system with internal circulation of the drying medium. *J. Food Process Eng.* **2020**, *43*, e13476.
18. Papastefanakis, N.; Daliakopoulos, I.N.; Maragkaki, A.E.; et al. Application of solar drying as a pre-treatment method for storing wet feedstocks prior to use in anaerobic digesters: Effect on methane production and digestate composition. *Fuel* **2023**, *348*, 128477.

19. Yao, L.S.; Song, Z.L.; Sun, C.G.; et al. Study on the evolution of internal and external water of lignite during microwave drying and the moisture reabsorption characteristics of dried lignite. *Energy Source Part A* **2025**, *47*, 3284–3301.
20. Idris, A.; Khalid, K.; Omar, W. Drying of silica sludge using microwave heating. *Appl. Therm. Eng.* **2004**, *24*, 905–918.
21. Savvakis, N.; Tournaki, S.; Tarasi, D.; et al. Environmental effects from the use of traditional biomass for heating in rural areas: A case study of Anogeia, Crete. *Environ. Dev. Sustain.* **2022**, *4*, 5473–5495.
22. Savvakis, N.; Sifakis, N.; Kotakidis, X.; et al. Multiple energy resources integration in the food industry: A technoeconomic analysis. *J. Clean Prod.* **2023**, *426*, 139055.
23. Guo, X.J.; Hao, Q.D.; Qiao, X.G.; et al. An evaluation of different pretreatment methods of hot-air drying of garlic: Drying characteristics, energy consumption and quality properties. *LWT-Food Sci. Technol.* **2023**, *180*, 114685.
24. Martynenko, A.; Bashkir, I.; Kudra, T. The energy efficiency of electrohydrodynamic (EHD) drying of foods. *Trends Food Sci. Tech.* **2021**, *118A*, 744–764.
25. Al Katsaprakakis, D.; Moschovos, T.; Michopoulos, A; et al. Feasibility for the introduction of decentralised combined heat and power plants in agricultural processes. A case study for the heating of algae cultivation ponds. *Sustain. Energy Technol.* **2022**, *53*, 102757.
26. Arnaoutakis, G.E.; Papadakis, N.; Al Katsaprakakis, D; et al. CombiCSP: A python routine for dynamic modeling of concentrating solar power plants. *Softw. Impacts* **2022**, *13*, 100367.
27. Arnaoutakis, G.E.; Katsaprakakis, D.A.; Christakis, D.G. Dynamic modeling of combined concentrating solar tower and parabolic trough for increased day-to-day performance. *Appl. Energy* **2022**, *323*, 119450.
28. Ahmad, F.Z.; Kashif, M.; Zhao, W.K.; et al. Microwave Heating Performances of Eucalyptus Camaldulensis Leaves with Silicon Carbide for Biofuel Upgrading. *Green Energy Fuel Res.* **2025**, *2*, 1–12.
29. Alfiya, P.V.; Jayashree, E.; Anees, K. Techno-economic, environmental impact and exergy analysis of microwave assisted drying of nutmeg mace. *Environ. Prog. Sustain.* **2025**, *44*, e14550.
30. Wang, J.; Wen, M.Y.; Ren, J.R.; et al. Tailoring microwave frequencies for high-efficiency hydrogen production from biomass, *Energy* **2024**, *297*, 131337.
31. Ahmad, F.; Zhang, Y.N.; Fu, W.M.; et al. Microwave-assisted chemical looping gasification of sugarcane bagasse biomass using Fe_3O_4 as oxygen carrier for H_2/CO-rich syngas production. *Chem. Eng. J.* **2024**, *501*, 157675.
32. Ozdemir, M.; Sakine, K. Effects of microwave drying on physicochemical characteristics, microstructure, and antioxidant properties of propolis extract. *J. Sci. Food. Agric.* **2023**, *104*, 2189–2197.
33. Carvalho, G.R.; Monteiro, R.L.; Laurindo, J.B.; et al. Microwave and microwave-vacuum drying as alternatives to convective drying in barley malt processing. *Innov. Food Sci. Emerg.* **2021**, *73*, 102770.
34. Wang, G.Y.; Zhang, K.; Huang, B.C.; et al. Microwave Drying of Sewage Sludge: Process Performance and Energy Consumption. *Processes* **2024**, *12*, 432.
35. Slezak, M.; Migas, P.; Bernasowski, M. The use of microwave treatment as a sustainable technology for the drying of metallurgical sludge. *Materials* **2024**, *17*, 6207.
36. Wulyapash, W.; Phongphiphat, A.; Towprayoon, S. Comparative study of hot air drying and microwave drying for dewatered sludge. *Clean Technol. Environ.* **2022**, *24*, 423–436.
37. Liu, C.Y.; Liu, Z.H.; Zhang, M.; et al. Drying of industrial sludge using microwave: Heating performance, mass loss, and energy analysis. *Biomass Bioenergy* **2025**, *197*, 107794.
38. Kodom, P.; Aragón-Barroso, A.J.; Koledzi, E.K.; et al. Microwave Treatment of Three Different Types of Sewage Sludge Based on Their Solar Drying Exposure Time: Effect on Microorganisms, Water Content and Agronomic Aspects. *Water* **2024**, *16*, 321.
39. Kocbek, E.; Garcia, H.A.; Hooijmans, C.M.; et al. Effects of the sludge physical-chemical properties on its microwave drying performance, *Sci. Total. Environ.* **2022**, *828*, 154142.
40. Li, L.Z.; Jiang, X.W.; Qin, X.M.; et al. Experimental study and energy analysis on microwave-assisted lignite drying. *Dry Technol.* **2019**, *37*, 962–975.
41. Guo, J.L.; Zheng, L.; Li, Z.F. Microwave drying behavior, energy consumption, and mathematical modeling of sewage sludge in a novel pilot-scale microwave drying system. *Sci. Total Environ.* **2021**, *777*, 146109.
42. Jie, E.; Zhao, X.; Liu, G.; et al. Effects analysis on optimal microwave energy consumption in the heating process of composite regeneration for the diesel particulate filter. *Appl. Energy* **2019**, *254*, 113736.
43. Ke, C.F.; Liu, T.; Zhang, Y.N.; et al. Energy absorption performances of silicon carbide particles during microwave heating process. *Chem. Eng. Process* **2022**, *172*, 108796.
44. Gong, Z.Q.; Zhang, H.T.; Liu, C. et al. Co-Pyrolysis Characteristics and Kinetic Analysis of Oil Sludge with Different Additives. *J. Therm. Sci.* **2021**, *30*, 1452–1467.
45. Liu, Q.W.; Liu, M.M.; Zhao, K.; et al. Microwave Application in Biomass Conversion: A Review. *ChemBioEng Rev.* **2024**, *11*, e202400020.

46. Ito, S.; Huang, H.Y.; Watanabe, F.J.; et al. Heat transfer during microwave-assisted desorption of water vapor from zeolite packed bed. *Dry Technol.* **2012**, *30*, 1707–1713.
47. Luo, R.; Tu, C.Z. Actual diffusivities and diffusion paths of water vapor in asphalt mixtures. *Constr. Build. Mater.* **2019**, *207*, 145–157.
48. Guan, B.W.; Cao, X.H.; Wang, A.P.; et al. Investigation on void connectivity characteristics of steel slag asphalt mixture subjected to dry-wet cycles and microwave heating utilizing computed tomography technology. *Mater. Struct.* **2025**, *58*, 47.